Review

ACTIVATION OF INFLAMMATORY MEDIATORS, MICROGLIA AND ASTROCYTES AFTER EXPERIMENTAL TRAUMA TO THE IMMATURE RAT BRAIN

Vanya Goranova, Marco Sifringer[1], Chrysanthy Ikonomidou[2]

Department of Anatomy, Histology and Embryology, Varna Medical University
[1]Department of Neonatology, Virchow Klinikum Berlin, Germany
[2]Department of Pediatric Neurology, Medical Faculty Carl Gustav Carus, Dresden, Germany

Summary

Mechanical brain trauma in infant rats produces an acute excitotoxic lesion at the impact site and delayed apoptotic degeneration associated with activation of inflammatory mediators. Apoptotic cell death, as demonstrated by TUNEL, affects mostly neuronal populations in the cortex, thalamus and caudate nucleus mainly ipsilateral to the injury 6 hours to 5 days later. We studied the timely expression of two inflammatory cytokines, interleukin (IL)-1ß and IL-18, 2 hours to 14 days following trauma. A detailed analysis of the distribution patterns and numerical densities of microglia/astrocytes was performed, using immunohistochemistry and dissector stereology. Increased expression of IL-1ß/IL-18 and substantial activation of both cell types occurred at the site of primary and secondary damages. A marked increase of mRNA and protein levels for both interleukins was detected 2-12 hours after injury. Microglial activation was first evident at 12 hours, peaked at 36-48 hours and decreased significantly by 5 days. Astrocytic activation was initially detected at 18 hours, peaked at 48 hours and gradually declined by day 14 after trauma. The present findings suggest that activation of microglia/astrocytes and IL-1ß/IL-18 might help sustain apoptotic neurodegeneration over several days following trauma to the immature brain.

Key words: trauma, apoptotic neurodegeneration, inflammation, cytokines

Introduction

Traumatic brain injury (TBI) is a common cause of mortality and developmental disability in childhood [1]. Clinical and experimental evidence suggests that the immature brain is unique in its response and vulnerability to TBI compared to the adult brain [2]. Recent clinical and experimental data indicate that apoptosis, inflammation and oxidative stress play a major role in the pathogenesis of neuronal death following TBI. Neuronal apoptosis occurs during normal development, but also in many neurodegenerative diseases and injuries to the central nervous system (CNS). Physiological apoptosis in the developing brain and active cell

Corresponding author:
Vanya Goranova
Department of Anatomy,
Histology and Embryology,
Varna Medical University,
55 Marin Drinov Str.,
9002 Varna,
Bulgaria;
e-mail: vanya.goranova@mu-varna.bg

Received: July 28, 2009
Revision received: November 19, 2009
Accepted: December 14, 2009

death in the adult brain share similar molecular mechanisms [3]. Neuroinflammation represents a potential pathogenetic factor in many CNS disorders, including brain trauma [4]. Macrophage accumulation, microglia activation and reactive astrogliosis are well-known to occur following brain trauma [5, 6]. Microglia and astrocytes are involved in inflammatory events after brain injury [7, 8]. However, their controversial roles in the developmental TBI still remain to be elucidated. Previously, we demonstrated that mechanical trauma to the immature brain causes acute excitotoxic cell death in the area of impact that is followed by massive delayed apoptosis in many brain regions ipsi- and contralateral to the trauma site [9]. The present study investigates the time course, morpholpogical appearance and topography of microglia and astrocytes in reponse to apoptotic neurodegeneration, as well as their association with the expression of two inflammatory cytokines IL-1ß and IL-18, following trauma to the infant brain.

Material and Methods

Animals, trauma and tissue sampling

All animal experiments were done in accordance with institutional guidelines. Seven-day-old Wistar rat pups (BgVV, Berlin, Germany), were subjected to head trauma as previously described [9]. After trauma or sham surgery, animals survived 6, 12, 18, 24, 36, 48 h or 5, 14, 21 days (n=5 per time point) and were then transcardially perfused with 0.01M PBS, followed by 4% paraformaldehyde in 0.1M PB. The whole brains were removed and post-fixed in the same fixative.

For RT-PCR and Western blotting, animals were sacrificed at 2, 6, 12, 24, 48, 72 h, 7 and 14 days later (n=4-5 per time point). Fresh tissue was prepared from cortex, striatum and thalamus, subsequently snap frozen in liquid nitrogen and stored at -80°C until analysis.

Histological processing and staining

Postfixed brains were embedded in paraffin. Coronal sections, 6-10 µm thick, were cut and processed for common staining or specific peroxidase labelling. Terminal deoxynucleotidyl transferase-mediated deoxyuridine triphosphate nick end labeling (TUNEL) using ApopTag Peroxidase *In Situ* Apoptosis Detection kit (Oncor Appligene, Heidelberg, Germany) was performed to detect apoptosis. Glial fibrillary acidic protein (GFAP), which is an intermediate filament protein expressed by mature astrocytes, was detected using an anti-GFAP rabbit polyclonal antibody (AB) (Chemicon International, Temecula, CA). Peroxidase conjugated Griffonia simplicifolia isolectin-B_4 (GSA I-B_4) (Sigma, St. Louis, MO) was used for evaluation of microglia. Double staining for TUNEL and GSA I-B_4, TUNEL and GFAP or GFAP and GSA I-B_4 was performed in representative sections. Anti-IL-1ß goat polyclonal AB or anti-IL-18 goat polyclonal AB (both from Santa Cruz Biotechnology, Santa Cruz, CA) were applied to detect IL-1ß and IL-18. In brief, each staining procedure included most of the following steps: 1. Pretreatment with 20 µg/ml proteinase K (Sigma, Saint Louis, MO) in 0.05M Tris buffer, pH 7.4, over 15 min at room temperature (RT) for TUNEL, GSA I-B_4, and GFAP or in 0.01M citrate buffer, pH 6.0 in microwave for 10 min for IL-1ß/IL-18. 2. Inactivation of the endogenous peroxidase with 3% H_2O_2 in absolute methanol for 20 min. Additionally, sections for GFAP were incubated with avidin for 15 min, then with biotin for 15 min (Avidin/Biotin blocking kit, Vector Laboratories, Burlingame, CA), followed by incubation in 1% bovine albumin (Sigma) for 1 h at RT to block nonspecific sites. For IL-1ß and IL-18 labelings, sections were incubated in blocking solution with 10% normal horse serum (Vector Laboratories) containing 1% albumin from bovine serum (Sigma) for 30 min at RT. 3. Incubation with specific agents or antibodies was performed for TUNEL in equilibration buffer for 20 min followed by working strength TdT enzyme for 1 h at 37°C, then in working strength stop/wash buffer for 30 min at 37°C, followed by anti-digoxigenin-peroxidase conjugate for 30 min at RT. Sections for GSA I-B_4 were incubated with peroxidase conjugated GSA I-B_4, 2µg/ml for 20 h at 4°C. Anti-GFAP rabbit polyclonal AB (1:500, Chemicon International) in 0.1% BSA for 20 h at 4°C or anti-IL-1ß goat polyclonal AB (1:500, Santa Cruz Biotechnology) or anti-IL-18 goat polyclonal AB (1:200, Santa Cruz Biotechnology) both overnight at 4°C. 4. Sections were then incubated with biotinylated goat anti-rabbit IgG (1:200, Vector Laboratories) for GFAP detection or horse anti-goat IgG (1:200, Vector Laboratories) for IL -1ß/IL -18

detection for 1 h at RT followed by ABC reagent (ABC Elite Standard Kit, Vector Laboratories) for 30 min at RT. 5. Individual substrates were then applied. By TUNEL, GSA I-B_4, and GFAP staining it was 0.05% 3,3'-diaminobenzidine tetrahydrochloride (DAB, Sigma) in 0.05M Tris buffer with 6.7% Imidazol (Sigma) and 0.02% H_2O_2 for 8-10 min. As second labelling system for TUNEL and GSA I-B_4, TUNEL and GFAP or GFAP and GSA I-B_4, we used peroxidase-based SG substrate (SG substrate kit, Vector Laboratories) or alkaline phosphatase-based VR substrate (VR substrate kit, Vector Laboratories). By IL-1ß or IL-18 staining, Vector Nova Red (VNR) substrate (Vector Laboratories) was applied for 7-8 min. **6.** Most of the sections for TUNEL, GSA I-B_4, and GFAP stainings, were counterstained with 0.5% methyl green and those for IL -1ß/IL -18 in hematoxylin (Gill's formula) (both from Vector Laboratories). Between incubation steps, sections were washed in 0.01M PBS, pH 7.4 in 0.1% Triton X-100 (Sigma), except for TUNEL in 0.05M PBS, pH 7.4 and IL -1ß/IL-18 in 0.01M PBS, pH 7.4. **7.** Finally, sections were dehydrated in ascending ethanol series, cleared in xylene and mounted with permount mounting medium. For each staining, parallel negative reagent controls were performed by omitting first or secondary Abs/reagents. Positive tissue controls were also done using sections on slides provided by the companies supplying first Abs/kits or known as positive from our previous experiments. Sections were analysed with an Olympus BX60 system microscope. Digital images were collected using a Zeiss Axioplan 2 microscope and a Nikon Coolpix 990 camera.

Semiquantitative RT-PCR and immunoblotting for IL-1ß/IL-18

Total cellular RNA was isolated from snap frozen tissue by acidic phenol/chloroform extraction and DNAse I treatment (Roche Diagnostics, Mannheim, Germany), RNA was reverse transcribed and the resulting cDNA was amplified by PCR. Protein extracts were obtained from homogenized snap frozen tissue, then centrifuged, denaturated and electrotransferred onto a nitrocellulose membrane. It was incubated with anti-IL-1ß goat polyclonal AB (Santa Cruz Biotechnology) or anti-IL-18 AB goat polyclonal AB (R&D Systems, Minneapolis, MN) respectively. Membranes were incubated with stripping buffer, then washed, blocked, and reprobed with anti-ß-actin mouse monoclonal AB (Sigma).

Morphometric and statistical analyses

Morphometric analysis was performed to evaluate TUNEL(+) nuclei, GSA I-B_4(+) microglia and GFAP(+) astrocytes in two brain regions, frontal cortex and dorsolateral thalamus, using an unbiased stereological method as previously described [9]. Counting was done in a blinded fashion. Values are presented as mean ± S.E.M. Comparisons among groups were made using one-way ANOVA with Newman-Keul's post-hoc test or unpaired Student´s t-test.

Results

Distribution and timely evolution of apoptotic neurodegeneration after cortical trauma

In 8-day-old control rats, few TUNEL(+) cells were detected within the cortex, thalamus (Fig. 1A, C), striatum, hippocampus and white matter tracts around the lateral ventricles. After trauma, increased densities of apoptotic cells were detected in striatum, cingulate/retrosplenial and frontoparitetal cortex starting at 6 h later. Apoptotic degeneration was further significantly increased in those areas at 12 h, and in addition spread to dorsolateral and ventromedial parts of the thalamus, hippocampal dentate gyrus and subiculum. Cingulate (Fig. 1B), frontal, retrosplenial and parietal cortices, thalamic nuclei (Fig. 1D), caudate, dentate gyrus and subiculum were most severely affected. TUNEL staining was more readily detectable ipsilaterally to trauma, and though to a lesser extent, in the contralateral site at 6 h, reached a peak at 24 h, declined significantly by 48 h (Fig. 4). At day 5, it did not significantly differ from those in control rats. Neuronal apoptosis in the neocortex was most pronounced in layers II and IV. Double labelling for TUNEL and GSA I-B_4 or TUNEL and GFAP at 24, 36 and 48 h after trauma revealed that the vast majority of apoptotic cells were GSA I-B_4(-) and GFAP(-).

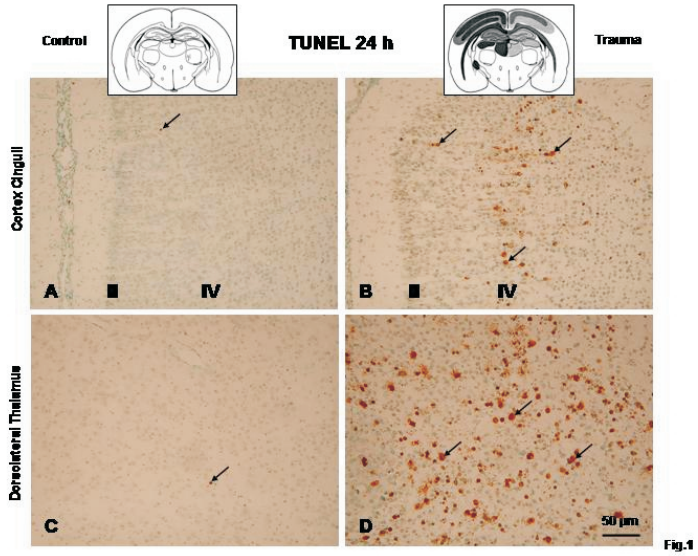

Fig. 1. Light micrographs showing TUNEL(+) nuclei (arrows). In control animals (**A, C**) only few TUNEL(+) profiles are found, whereas massive apoptotic neurodegeneration is seen at 24 h after trauma mainly in layers II and IV of the cortex (**B**) and thalamus (**D**) ipsilateral to the injury. DAB substrate, methyl green counterstaining.

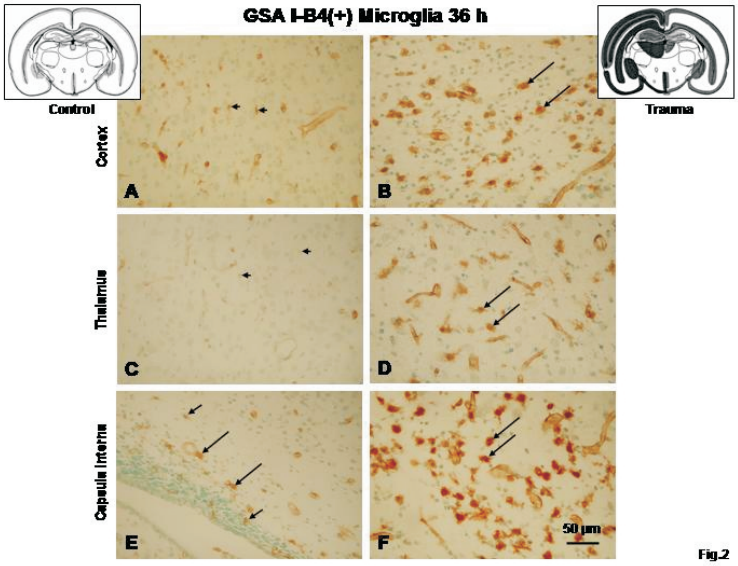

Fig. 2. Light micrographs showing GSA I-B_4(+) microglia. In control animals (**A, C, E**), there were ramified microglia (short arrows) in cortex (**A**) and thalamus (**C**). Amoeboid microglia (long arrows) and cells with a mixed phenotype (medium arrows) are present in small numbers in white matter tracts and at the border zones with the gray matter (**E**). After trauma, amoeboid microglia increase substantially in number in the ipsilateral cortex (**B**), thalamus (**D**) and in all white matter tracts (**F**) reaching a maximum by 36-48 h. DAB substrate, methyl green counterstaining.

Acute activation of microglia and astrocytes by TBI

Trauma induced strong activation of both microglia and astrocytes. In control 8-day-old rats, GSA I-B_4 labeled microglia demonstrated two phenotypes, ramified and amoeboid. Ramified microglia were elongated cells with a small cell body but long and well-branched processes distributed mainly throughout the gray matter (Fig. 2A, C). Amoeboid microglia were oval or round cells with relatively short and thick processes found in small quantities mainly within white matter tracts (Fig. 2E). We also found cells with a mixed phenotype and characteristics of both of the above types, distributed scarsely in the gray matter or at the border zones between gray and white matter (Fig. 2E). Following head trauma, increased numbers of amoeboid and transitional microglia were found within cortical contusion area and at distant sites, severely affected by apoptotic neurodegeneration, such as cortex, striatum, hippocampus, thalamus and white matter tracts (Fig. 2B, D, F). This activation started at 12 h after trauma, peaked by 36-48 h (Fig. 4) and decreased significantly by day 5.

In 8-day-old control animals, GFAP(+) cells were usually present mainly in white matter tracts, within the molecular cortical layer and in the border zones between gray and white matter (Fig. 3A, C, E). Initially, a significant increase in the densities of GFAP immunoreactive astrocytes (hyperplasia) and an obvious increase

in intensity of staining (hypertrophy) were first detected within the corpus callosum and cortex by 18 h after trauma. Maximal GFAP staining and highest numerical densities of GFAP(+) cells were found at 48 h after trauma (Figs. 3B, D, F; 4). Astrocytic activation was observed in the same regions in which apoptotic cell death took place, including white matter tracts. It decreased significantly by 5 days after trauma but was still present on day 14.

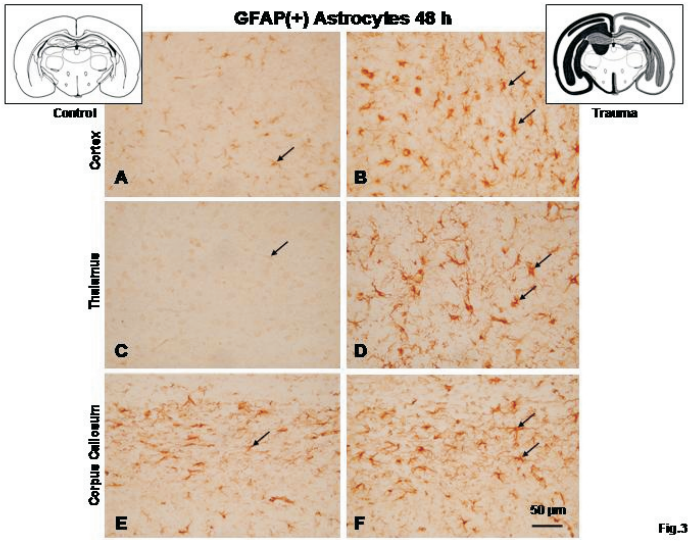

Fig. 3. Light micrographs showing GFAP(+) astrocytes (arrows). In control rats they are distributed in white matter tracts and at the border-zones to the gray matter (**A, C, E**). The numbers of GFAP(+) astrocytes reached a maximum 48 h after trauma in the primary and secondary lesioned areas such as cortex retrosplenialis II-IV (**B**) and thalamus (**D**) and in the white matter tracts (**F**) ipsilateral to the trauma site. DAB substrate.

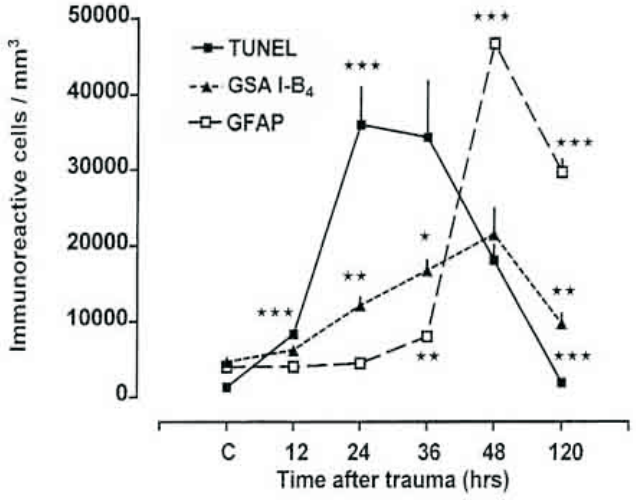

Fig. 4. Mean numerical densities (SEM's) of TUNEL(+) cells, GSA I-B_4(+) microglia and GFAP(+) astrocytes in dorsolateral thalamus ipsilateral to trauma site in control 7-day-old rats at 12 h, 24 h, 36 h, 48 h and 120 h (n=5 for each group). The numerical density at a given time point is compared to the density at the previous time point on the curve for each cell type by means of Student's t-test (*P<0.05, **P<0.01, ***P<0.001).

Increased expression of IL-1ß and IL-18 after TBI

Levels of IL-1ß and IL-18 mRNA were significantly elevated in thalamus and cortex ipsilateral to the trauma site at 6 h and remained elevated for up to 24 h for IL-1ß and 72 h for IL-18 (Fig. 5A, B). Two way ANOVA revealed that trauma had a highly significant effect on IL-1ß and IL-18 mRNA levels in brain areas analyzed (Fig. 5C, D). Elevation of IL-18 mRNA levels occurs in a more delayed fashion compared to IL-1ß (IL-1ß at 2 h, ***P<0.001), with a highly significant elevation at 12 h ***P<0.001, as determined by ANOVA. Densitometric analysis of Western blots for IL-1ß and IL-18 protein revealed a significant increase of both proteins at 6 hours (*P<0.05 as analyzed by ANOVA Fig. 6A, B, C). IL-1ß protein decreased by 72 h, whereas IL-18 protein levels remained high for 3 days after the insult. A significant decrease of IL-18 protein back to normal levels was observed by 7 days after trauma (Fig. 6 C). Immunopositive cells for IL-1ß and IL-18 were first detected at 12 h after TBI mainly at the trauma site but also in distant cortical areas, thalamus, striatum and white matter tracts. Some cells were most probably blood-derived neutrophils and monocytes/macrophages, as well as activated

local microglia, reactive astrocytes and endothelial cells. The number of IL-1ß (+) cells reached a peak at 24-36 h for (Fig. 6 D) and for IL-18 (+) cells at 36-48 h (Fig. 6 E). Thereafter, both immunopositivities declined to insignificant levels by day 5-14 following trauma.

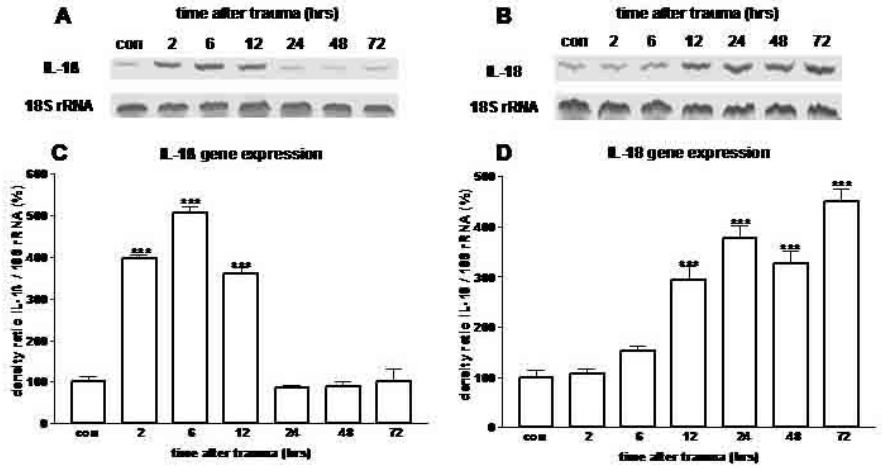

Fig. 5. Increased mRNA expression of IL-1ß and IL-18 in the parietal cortex ipsilateral to the trauma site. In the upper panels, increased mRNA expression for IL-1ß **(A)** and IL-18 **(B)** is shown in polyacrylamide gels by semiquantitative RT-PCR, 2-72 hrs after trauma. No change in the expression of 18S rRNA is detected. The histograms demonstrate a significant increase in the mRNA levels for IL-1ß **(C)** and IL-18 **(D)**, as detected by semiquantitative RT-PCR, compared to control group (con), (***P<0.001, ANOVA).

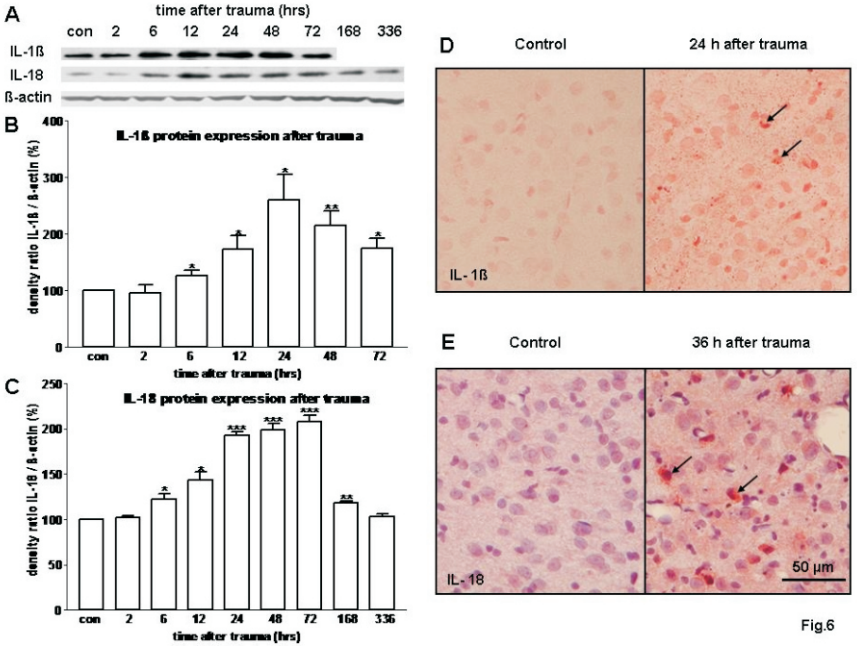

Fig. 6. Increased protein expression for IL-1ß and IL-18 ipsilaterally to trauma site 6-72 h without change in the levels of ß-actin **(A)**. Densitometric analysis revealed a significant increase of IL-1ß and IL-18 proteins at 6 hours **(B, C)**. Densitometric data represent the density ratio of the respective bands to the corresponding ß-actin band. Data are compared to control group (con) (control=100%, *P<0.05, **P<0.01, ***P<0.001, one-way ANOVA). Immunohistochemical staining for IL-1ß in the ipsilateral thalamus 24 h after trauma **(D)** and for IL-18 36 h after trauma **(E)**. In control animals immunopositive cells are normally absent in the thalamus but appear in large numbers after TBI (arrows). VNR substrate **(D, E)** and hematoxylin counterstaining **(E)**.

Discussion

Our results illustrate the time course and topography of microglial/astroglial activation in association with IL-1ß/IL-18 expression mainly ipsilateral to trauma site in gray and white matter, as well as in distant regions that suffer apoptotic neurodegeneration - cortex, thalamus and other gray matter areas.

Microglial phenotypes, microglial activation as a result of trauma-induced neuronal apoptosis

In control animals, we found a small number of amoeboid microglia localized mainly in the white matter, whereas in the gray matter microglia were of transitional or resting phenotype. They show loss of surface carbohydrate residues and down-regulation of markers characteristic for cells of the monocyte-macrophage series [10]. Trauma induces a strong and rapid increase in the number of the amoeboid forms, probably due to hyperplasia and transformation of resting microglia into reactive and phagocytic cells. Shortly after trauma, we detected a large number of amoeboid and highly ramified transitional microglia engulfing cellular debris in the peritraumatic region in close association with the area of cortical necrosis. Recently, using time-lapse transcranial two-photon imaging of GFP-labelled microglia *in vivo,* it has been shown that the presumed resting microglia are highly active in their resting state and become rapidly activated upon injury [11].We consider that most of the lectin(+) cells at the lesion site are blood-derived monocytes/macrophages. Our findings do not indicate a causative role of microglia in initiation of apoptotic neurodegeneration but show that up to 5 days after trauma, i.e., the period of microglial activation, apoptotic neurodegeneration is continuously ongoing. This suggests the possibility that, once activated, microglial cells may entertain the apoptotic process by secreting neurotoxins and other promoting factors, including cytokines [4].

Significance of post-traumatic reactive astrogliosis

Usually, different forms of brain injury elicit reactive gliosis, characterized by hyperplasia and cellular hypertrophy of both microglia and astrocytes. Astrogliosis represents a shared feature of acute and chronic neurodegenerative diseases with an inflammatory component. It is characterized by increased expression of GFAP and emission of GFAP(+) processes. We found a close spatial and temporal correlation between the activation patterns of microglia and astroglia. However, astroglial response follows microglial activation by several hours. This is suggestive of a possible interaction between these two glial cell types. Activated microglia are known as secretors of astroglia-stimulating factors, whereas astroglia produce mitogenic factors and other substances modulating microglial inflammatory response. In the last 10 years, accumulating data strongly suggest a neuroprotective role of microglia in acute CNS injuries as opposed to chronic CNS diseases with slowly progressing neurodegeneration [12]. Recent evidence suggest that astroglial reactivity promotes CNS recovery and repair [13], as astrocytes produce a range of trophic factors that aid survival of both neurons and oligodendrocytes. Therefore, we consider the spatial and temporal evolution patterns of microglial and astroglial responses to TBI are not suggestive of a causative role of either of the two cell types in the pathogenesis of apoptotic cell death in this infant trauma model. Their activation rather represents a response to an already initiated cell death process. Although both cell types may contribute to tissue destruction after CNS injuries, blockade of their activation may exert negative effects on overall tissue repair and plasticity. In our study, we found a longer lasting astrocytic activation that was still evident on day 14 after trauma, as compared with shorter effects of microglia and interleukins. This is highly suggestive of a possible involvement of reactive astrocytes most probably in reparative processes rather than in destructive events at such longer time points after trauma.

Increased expression of the pro-inflammatory cytokines IL-1ß and IL-18

Here we present evidence that TBI-induced microglial/astroglial activation is accompanied by increased expression of pro-inflammatory cytokines IL-1ß and IL-18. The initial upregulation at their mRNA and protein levels is followed by the presence of a large number of immunopositive cells at the impact site and in areas with pronounced apoptotic cell death, such as thalamic nuclei and cortex. The distribution

pattern and time course of expression of both IL-1ß and IL-18 immunomarkers within the gray and white matter were very similar, but with a delay of 12 h for IL-18. The location and temporal expression of IL-1ß/IL-18 immunopositive cells at the site of primary lesion in the parietal cortex and in the sites of apoptotic neurodegeneration coincided with the maximal activation of local microglia and astrocytes detected in our experiment. IL-1ß was more strongly expressed at the trauma site, whereas IL-18 was mostly found in the areas of apoptotic neurodegeneration over a longer time period as compared to Il-1ß. Our data are more suggestive of a beneficial role of both interleukins as mediators of cellular interaction in the injured immature brain.

Conclusions

In the developing brain, trauma-induced neuronal apoptosis provokes a strong activation of microglia and astroglia. Microglial response is closely followed by post-traumatic reactive astrogliosis. Activation of microglia/astrocytes leads to a local and systemic increase of the pro-inflammatory cytokines IL-1ß and IL-18. These events might help sustain apoptotic neurodegeneration over several days following trauma but they might promote also tissue repair in the injured immature brain. Understanding the precise contribution of both glial cell types to progression of apoptotic neurodegeneration, inflammation and tissue repair in the developing brain may provide valuable information to guide treatment of pediatric head trauma patients.

Acknowledgements

This work was supported by DFG grant IK2/5-1 and IK2/5-2

References

1. Anderson V, Cartroppa C, Morse S, Haritou F, Rosenfeld J. Functional plasticity or vulnerability after early brain injury? *Pediatrics*. 2005;116:1374-1382.
2. Kochanek PM. Pediatric traumatic brain injury: quo vadis? *Dev Neurosci*. 2006;28:244-255.
3. Yuan J, Yankner BA. Apoptosis in the nervous system. *Nature*. 2000;407:802-807.
4. Holmin S, Höjeberg B. In situ detection of intracerebral cytokine expression after human brain contusion. *Neurosci Lett*. 2004;369:108-114.
5. Tatsumi K, Haga S, Matsuyoshi H, Inoue M, Manabe T, Makinodan M et al. Characterization of cells with proliferative activity after brain injury. *Neurochem Intern*. 2005;46:381-389.
6. Zhang Z, Artelt M, Burnet M, Trautmann K. Early infiltration of macrophages/microglial to rat traumatic brain injury. *Neuroscience*. 2006;141:637-644.
7. Lau LT, Yu AC. Astrocytes produce and release interleukin-1, interleukin-6, tumor necrotic factor alpha and interferon-gamma following traumatic and metabolic injury. *J. Neurotrauma*. 2001;18:351-359.
8. Chew LJ, Takanohashi A, Bell M. Microglia and inflammation: impact on developmental brain injuries. *MRDD Res Rev*. 2006;12:105-112.
9. Bittigau P, Sifringer M, Pohl D, Stadthaus D, Ishimaru M, Shimizu H et al. Apoptotic neurodegeneration following trauma is markedly enhanced in the immature brain. *Ann Neurol*. 1999;45:724-735.
10. Guillemin GJ, Brew BJ. Microglia, macrophages, perivascular microphages, and pericytes: a review of function and identification. *J Leukoc Biol*. 2004;75:388-397.
11. Nimmerjahn A, Kirchhoff F, Helmchen F. Resting microglial cells are highly dynamic surveillants of brain parenchyma in vivo. *Science*. 2005;308:1314-1318.
12. Streit WJ. Microglia as neuroprotective, immunocompetent cells of the CNS. *Glia*. 2002;40:133-139.
13. Liberto CM, Albrecht PJ, Herx LM, Yong VW. Pro-regenerative properties of cytokine-activated astrocytes. *J Neurochem*. 2004;89:1092-1100.